03,10,16

Interface anisotropy manifestation in CdTe/CdZnTe quantum wells

© L.V. Kotova[1], R. Andre[2], H. Mariette[2,3], V.P. Kochereshko[1]

[1] Ioffe Institute,
St. Petersburg, Russia
[2] Institut Neel CNRS,
Grenoble, France
[3] Japanese-French laboratory for Semiconductor Physics and Technology J-F AST,
CNRS, Universite Grenoble Alpes,
University of Tsukuba, Japan

E-mail: kotova@mail.ioffe.ru

Received May 11, 2023
Revised May 11, 2023
Accepted May 12, 2023

The spectra of polarized reflection from a structure with a single quantum well and asymmetric $Cd_{0.9}Zn_{0.1}Te/CdTe/Cd_{0.4}Mg_{0.6}Te$ barriers are studied in this work. The Stokes parameters of reflected light were measured. In the structure with asymmetric barriers under study in the region of exciton resonances, the phenomenon of light birefringence caused by a reduced symmetry of the interfaces compared to the bulk was found.

Keywords: quantum well, excitons, anisotropy, interface.

DOI: 10.61011/PSS.2023.07.56412.80

1. Introduction

Having high structural perfection and unique optical properties, semiconductor compounds $A^{II}B^{VI}$, in particular CdTe and ZnTe, are primarily used as a model for investigation of new physical phenomena. Unfortunately, they have not been widely used yet for various applications due to their fast degradation. One of the reasons hindering the practical use of heterostructures based on CdTe and ZnTe compounds is the noticeable mismatch of their crystal lattices. As a result, mechanical stresses arise at the interfaces and can lead to the destruction of the structure [1].

Currently, $A^{II}B^{VI}$ compounds are increasingly considered as promising materials for solar power [2]. CdTe is one of the leading materials used in thin-film photovoltaic (PV) devices thanks to some of it main properties such as the ability to allow both *n*- and *p*-type doping, and relatively high photon absorption coefficient in the visible range. Direct band gap is $E_g \sim 1.514$ eV at room temperature which is close to the optimum band gap for solar energy conversion [3]. Despite the band gap close the optimum width, the highest energy conversion efficiency in CdTe solar cell which has been currently achieved using poly-crystalline CdTe amounts to 21% (this is much lower than the Shockley–Queisser limit $\sim 32\%$ for a single-junction cell). The investigations show that inclusion of $Cd_{1-x}Mg_xTe$ barrier in the solar cell structure may improve no-load voltage [4] and, finally, the cell performance.

Its is known empirically that „good" devices based on cubic semiconductors can be obtained, if they are made, for example, in direction [110] and „bad" devices - if they are made in the perpendicular direction. This is partially caused by the fact that these directions correspond to the dislocation development directions. But interfaces are exactly the place of maximum lattice mismatch in contacting materials and, therefore, a place of dislocation nucleation. Therefore investigation of the interface properties is essential practical task.

Thorough experimental study of polarized reflection spectra from a structure with quantum well and asymmetric barriers has been carried out herein. A birefringence phenomenon caused by low interface symmetry in the heterostructure has been detected. Low interface symmetry has been observed before in the photoluminescence spectra of type II heterostructures where the exciton is „tied" directly to the interface [5]. In this case, anisotropy manifested itself in the local properties of the structure. As opposed to [6,7], low interface symmetry manifested itself herein in the dielectric response of type I structures where the exciton is not tied to the interface, but is distributed throughout the quantum well. It is surprising that the exciton with its large radius can feel an atom structure of a separate interface with a thickness of one monoatomic layer.

2. Experiment

The experiment involved the investigation of $CdTe/Cd_{0.9}Zn_{0.1}Te$ structure with a single quantum well (QW) 8 nm in width grown in direction [001] by the molecular-beam epitaxy method. The structure was characterized by asymmetric barriers, one of which was $Cd_{0.9}Zn_{0.1}Te$ and the other barrier was based on $Cd_{0.4}Mg_{0.6}Te$ (Figure 1). The height of these barriers

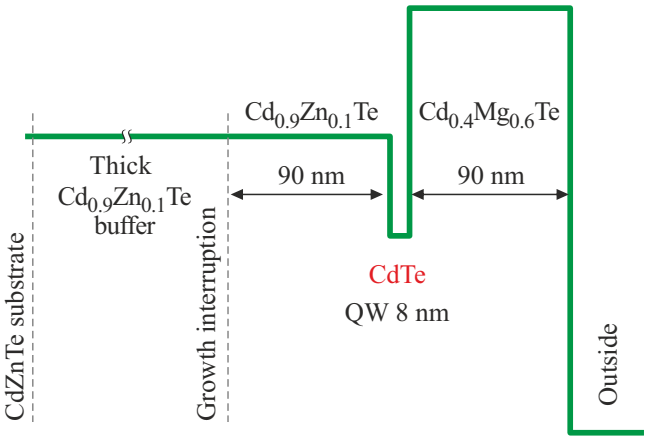

Figure 1. Test structure diagram. Heterostructure with a single 8 nm CdTe quantum well with asymmetric $Cd_{0.9}Zn_{0.1}Te$ and $Cd_{0.4}Mg_{0.6}Te$ barriers 90 nm in width each. Zn 10% buffer layer about 1 μm.

in thickness.

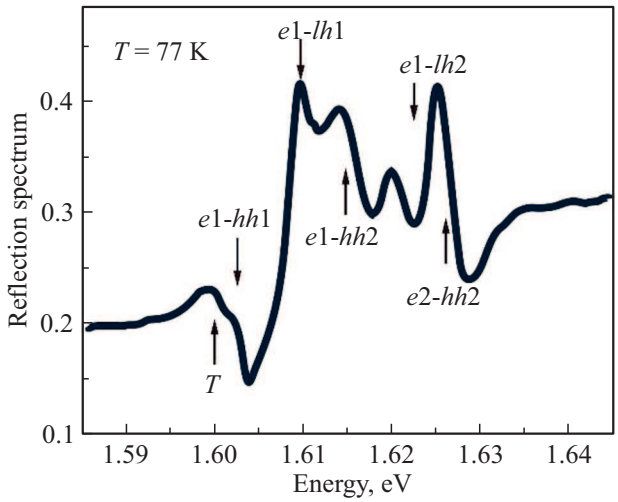

Figure 2. Reflection spectrum of the structure with a quantum well and asymmetric barriers recorded at 77 K. Arrows show optical transitions to exciton states with heavy and light holes. These transitions were identified on the basis of calculations, see the detailed description in [9].

differed by more than three times. The structure parameters are given in the caption to Figure 1. 1000 nm $Cd_{0.9}Zn_{0.1}Te$ was used as a buffer layer. The substrate was composed of Zn 4%. Owing to the thick buffer layer, the barrier layer turned out to be unstressed and all mechanical stresses were applied to the quantum well.

The reflection spectra were obtained using a monochromator with a focal distance of 0.5M and recorded by an CCD detector. To record the transmittance and reflection spectra, a halogen lamp was used as a light source.

Figure 2 shows a reflection spectrum of the structure. For the initial identification of lines in the reflection spectrum, we used the findings of [8], where the exciton reflection lineshape was analyzed. This study showed that the exciton reflection lineshape is determined by the interference of light reflected from the surface and QW. Depending on the phase shift when the light propagates from the surface to QW and back, the spectrum shape can change greatly.

It can have a maximum, minimum or „differential" shape — with the growing energy, the intensity first grows up to the maximum, then decreases to the minimum and than goes back to the middle level, or „inverse differential" shape — first minimum and then maximum [8]. This allowed to identify spectral peculiarities at 1.601, 1.604, 1.612 and 1.6.20 eV as related to different exciton states in the CdTe quantum well (Figure 2).

Polarized reflection spectra were also measured with normal and oblique light incidence on the structure. Conversion from linear to circular polarization was observed at oblique incidence. This phenomenon is associated with the quantum well gyrotropy and was thoroughly investigated in our previous studies [10,11]. In normal light incidence, polarization conversion was not observed in a structure with symmetric barriers, and in oblique light incidence, the circular polarization degree accounted for only a few percent [12]. Compared with this, the structure with asymmetric barriers showed a large conversion that achieved dozens of percent even in normal light incidence (Figure 3). The maximum circular polarization of the reflected light was observed when the incident light was linearly polarized along the [100] or [010] axes. If the incident light was polarized along the [110] or [1$\bar{1}$0] axes, the circular polarization of the reflected light was not higher than 2% (Figure 4).

Figure 3 shows the spectral dependences of the circular light polarization P_{cir} and linear polarization $P_{lin'}$

$$P_{cir} = \frac{R^{\sigma^+} - R^{\sigma^-}}{R^{\sigma^+} + R^{\sigma^-}}, \quad P_{lin'} = \frac{R^{x'} - R^{y'}}{R^{x'} + R^{y'}}. \qquad (1)$$

Spectral peculiarities of these dependences correspond to the spectral features of reflection spectra as shown by arrows in Figure 2. Note that minima in the dependence $P_{lin'}(\omega)$ correspond to zeros in the dependence $P_{cir}(\omega)$ as also follows from the equations for the circular and linear light polarization shown in Section „Discussion of findings".

Conversion of the linear light polarization to the circular polarization in this case is apparently associated with the birefringence phenomenon with the optic axis lying in the QW plane and directed along crystallographic directions [110] or [1$\bar{1}$0]. Deformation can actually result in the optical anisotropy and birefringence. However, despite the fact that the studied structures are actually stressed, these stresses cannot result in occurrence of a preferred axis in the structure plane. Actually, birefringence occurs only in an asymmetric structure and is not available in a symmetric structure at similar mechanical stresses [12]. It would appear reasonable that birefringence is associated with interface asymmetry, because the structures differ only in interfaces.

In [5], type II ZnSe/BeTe QW was used to show that in QW with symmetry D_{2d} based on cubic semiconductors

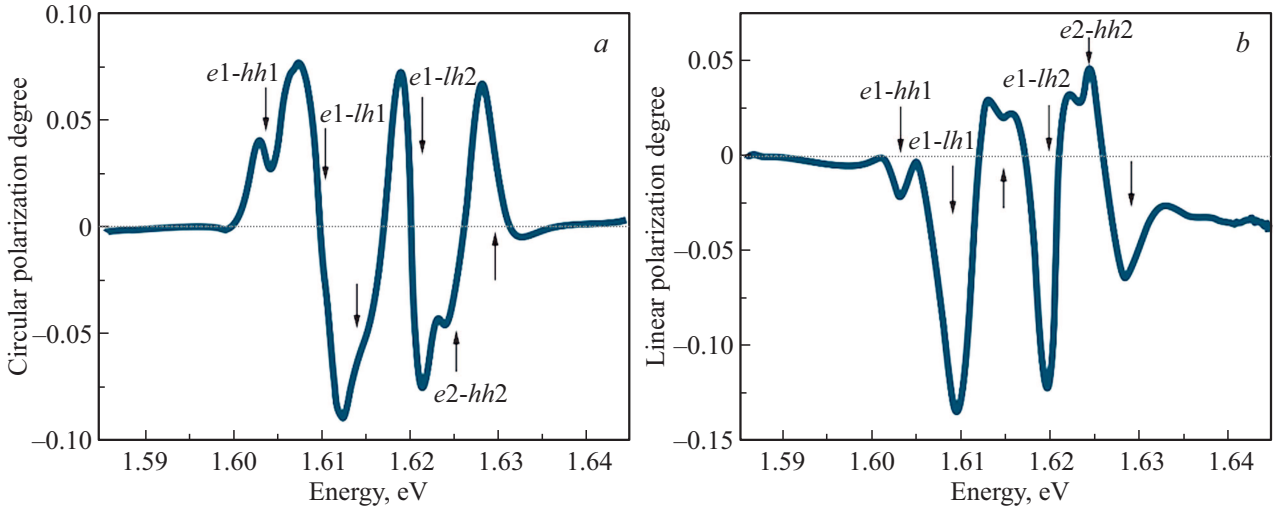

Figure 3. Polarization degree of light reflected from the structure with asymmetric barriers in normal light incidence linearly polarized in direction [100]. A) degree of circular polarization P_{cir}, B) degree of linear polarization in the [110] and [1$\bar{1}$0] axes turned at 45 degrees with respect to the incident light polarization $P_{lin'}$. The arrows show the peculiarities observed in the reflection spectrum (Figure 2).

with a zinc blende structure, the separate interface has symmetry C_{2v} with the second order axis in directions [110] or [1$\bar{1}$0]. Such low symmetry may result in the interfacial light birefringence in the exciton resonance region. However, at the second (opposite) interface in QW, the second order axis is always orthogonal to the axis at the first interface. Therefore, since in a common symmetrical QW, the exciton feels both interfaces in a similar way, the anisotropy of a separate interface does not appear. In our case, appearance of the optical anisotropy is associated with QW asymmetry, when the opposite interfaces are inherently different.

3. Discussion of findings

In the reflection spectra in Figure 2, a lot of peculiarities are observed, which is not typical of a structure with a single QW. The initial line identification in the spectrum was carried out by the lineshape of the exciton reflection from QW. The exciton reflection outline allows to determine the distance from the surface to QW [8] and identify which lines are related to the exciton in the well and which lines are related to other resonances. Indeed, the reflectance from the structure containing a quantum well r:

$$r = r_{01} + \frac{t_{01}t_{10}e^{2i\varphi}}{1 - r_{10}r_{QW}e^{2i\varphi}}\, r_{QW}. \qquad (2)$$

Here, t_{10} are the transmittances of the vacuum–crystal interface on the crystal side and t_{01} — on the vacuum side, r_{01} and r_{10} are the reflectances at the vacuum–crystal interface on the vacuum and crystal side, r_{QW} is the reflectance from QW, $\varphi = k(d + L/2)$ is the phase shift in light flow from the surface to the well, d is the thickness of the covering QW layer, k is the light wave vector.

Neglecting multiple reflections and a contribution quadratic in r_{QW}, we obtain the following for the observed reflectance

$$R = |r|^2 \approx R_0\left[1 + 2\,\frac{t_{01}t_{10}}{r_{01}}\,\mathrm{Re}\,\{r_{QW}e^{2i\varphi}\}\right]. \qquad (3)$$

Thus, the reflection spectrum shape is defined by the phase shift φ of light waves reflected from the surface and QW. The outer barrier thickness in the structure is 90 nm, the refraction index of light in CdMgTe in this spectral region is equal to $n \approx 2.45$. In this case the phase shift of the light wave passing through the barrier layer is approximately equal to $\pi/2$. This allows to identify the spectral peculiarities at 1.601, 1.604, 1.612 and 1.6.20 eV as related to different exciton resonances in QW (Figure 2) [8]. The lineshape of the exciton reflection from the CdZnTe barrier is the same as from the well (see Figure 2). Since this barrier is located at the same distance from the surface, the phase shift of the light wave reflected from the well and from the CdZnTe layer during the passage of the layer from the well to the surface is almost the same. For more thorough identification if line in the spectrum, energy levels and oscillator strengths of optical transitions to exciton states in QW were calculated [9]. Such identification is shown by arrows in Figures 2 and 3.

The amplitude reflectance of light from the quantum well in the vicinity of a single exciton resonance [13] is equal to

$$r = \frac{i\Gamma_0}{\omega_0 - \omega - i(\Gamma_0 + \Gamma)}, \qquad (4)$$

here Γ_0 is the radiation damping of exciton, Γ is the non-radiation damping of exciton, ω_0 is the resonance frequency of the exciton transition.

Let the light linearly polarized along the $x \parallel [100]$ and $y \parallel [010]$ axes falls on the sample surface along exis

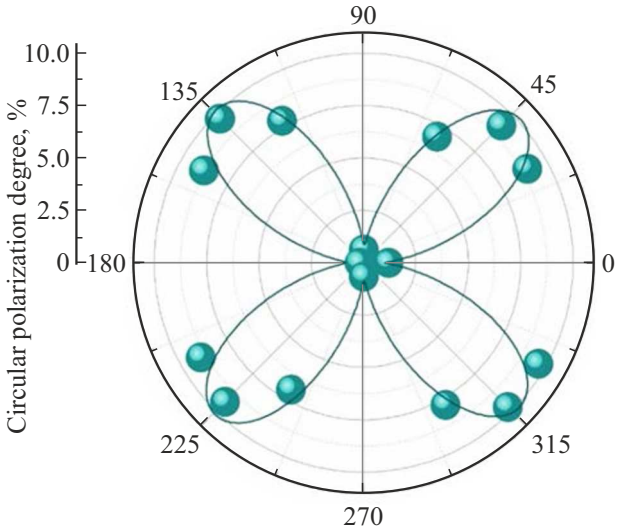

Figure 4. Dependence of the circular polarization degree of light reflected from the asymmetric structure with quantum well on the incident light polarization plane direction. The crystallographic axes [110] and [1$\bar{1}$0] correspond to directions 0 and 90 degrees, respectively.

$z \parallel [001]$. The degree of circular polarization of the reflected light

$$2iP_{cir} = r_x r_y^* - r_y r_x^*, \tag{5}$$

the $x' \parallel [110]$ and $y' \parallel [1\bar{1}0]$axes, $r_{x'}, r_{y'}$ are amplitude reflectances in the x' and y'axes.

The degree of linear polarization of the reflected light in the x' and y'axes turned at 45° with respect to the x and y axes:

$$2P_{lin'} = r_{x'} r_{y'}^* + r_{y'} r_{x'}^*. \tag{6}$$

The degree of linear polarization of the reflected light in the x and y axes:

$$2P_{lin} = r_x r_x^* - r_y r_y^*. \tag{7}$$

Due to the interface anisotropy in heterostructures [5,14], light and heavy hole states are mixed at the interface. As a result, the reflectances of light polarized along the [110] and [1$\bar{1}$0] axes in the exciton resonance region may differ greatly. The theory predicts that radiation dampings of exciton Γ_0 are different, while all other exciton parameters ω_0 and Γ are similar [15,16]. Then, for the circular polarization degree of light reflected from the structure, we obtain

$$P_{cir} = \frac{\Gamma_0^x \Gamma_0^y \Delta\omega(\tilde{\Gamma}^x - \tilde{\Gamma}^y)}{|\Delta\omega - i\tilde{\Gamma}^x|^2 |\Delta\omega - i\tilde{\Gamma}^y|^2}, \tag{8}$$

here $\Delta\omega = \omega_0 - \omega$, $\tilde{\Gamma} = (\Gamma_0 + \Gamma)$.

This equation shows that the degree of circular polarization P_{cir} vanishes at exciton frequencies. Whilst the maximum circular polarization degree of reflected signal is observed when the incident light is polarized along the $x \parallel [100]$ and $y \parallel [010]$ axes and the minimum polarization is observed for the light polarized along $x' \parallel [110]$ and $y' \parallel [1\bar{1}0]$ (Figure 4).

For the linear polarization degree in the x' and y' axes:

$$P_{lin'} = \frac{\Gamma_0^{x'} \Gamma_0^{y'} [(\Delta\omega)^2 + \tilde{\Gamma}^{x'} \tilde{\Gamma}^{y'}]}{|\Delta\omega - i\tilde{\Gamma}^{x'}|^2 |\Delta\omega - i\tilde{\Gamma}^{y'}|^2}. \tag{9}$$

It can be seen that the linear polarization degree in the turned axes does not change the sign and tends to zero away from the exciton resonances.

Let us estimate these values. From the experimental dependence (Figure 3) for the linear polarization $P_{lin'}(\omega)$, we obtain

$$P_{lin'} = \left(\frac{\Gamma_0^{x'}}{\tilde{\Gamma}^{x'}} \frac{\Gamma_0^{y}}{\tilde{\Gamma}^{y'}} \right) \approx 0.15.$$

Hence, $\frac{\langle\Gamma_0\rangle}{\langle\Gamma\rangle} \approx 0.387$. I.e. the non-radiation damping is approximately 3 times higher than the radiation damping. Similar value is also obtained from the reflectance spectrum (Figure 2). The line amplitude in the reflection spectrum is in fact approximately equal to $\frac{\langle\Gamma_0\rangle}{\langle\Gamma\rangle} \sim 0.5$.

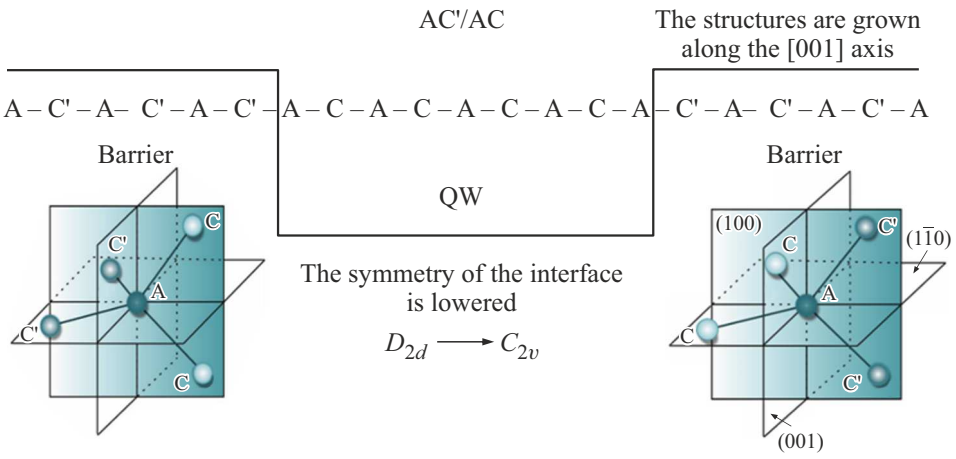

Figure 5. The interface structure near the heterotransition of two cubic semiconductors with the zinc blende symmetry having a common anion C′A/CA.

The maximum and minimum in the spectral dependence $P_{cir}(\omega)$ are spaced in frequency by $\Delta\omega \approx \Gamma$. Then it follows that

$$(P_{circ}^{\max} - P_{circ}^{\min}) \approx P_{lin'}^{\max} \frac{(\Gamma_0^x - \Gamma_0^y) + (\tilde{\Gamma}^x - \tilde{\Gamma}^y)}{2\langle\tilde{\Gamma}\rangle}. \qquad (10)$$

Hence $\Gamma_0^x/\Gamma_0^y \approx 2.5$. This value is close by the order of magnitude to that observed in type II ZnSe/BeTe quantum wells [14].

Such radiation damping anisotropy of the exciton is caused by mixing light and heavy hole states caused by low symmetry of a separate interface (C_{2v}) compared with the symmetry of the whole quantum well (D_{2d}). As shown in [5,7], the interfacial anisotropy occurs due to the orientation of chemical bonds in structures based on the zinc blende (Figure 5).

In crystals with the zinc blende structure, valence bonds are arranged along directions [110] or [1$\bar{1}$0]. As a result, heavy holes with a wave function, when passing through the interface, transform in light holes with the wave function $(X \mp iY) \pm 2Z$ [15,16]. This is manifested in the probability of optical transitions between the conduction band and hole states localized near the interfaces which is different for the light polarized along directions [110] and [1$\bar{1}$0].

In type II structures, electron and hole are in different layers, in this case the exciton is localized directly at the interface, and the interface anisotropy appears in local properties of the structure. In this case the interface anisotropy appears as the dielectric response anisotropy, i. e. in the macroscopic structure characteristic.

In symmetric structures, the exciton wave function „contacts“ both interfaces. Despite the low symmetry of each of the interface in the well, the exciton in this case „feels“ the symmetry of the whole well, i. e. D_{2d}. In the asymmetric structure, the interfaces are different and the exciton feels stronger only one of the barriers having the symmetry C_{2v}, i. e. the preferred axis [110] in the well plane.

4. Conclusions

Spectra of polarized reflection from the structure with type I quantum wells with asymmetric $Cd_{0.9}Zn_{0.1}Te/CdTe/Cd_{0.4}Mg_{0.6}Te$ barriers are investigated herein. The Stokes parameters of the reflected light were measured. In the structure with asymmetric barriers, light birefringence phenomenon was detected in the exciton resonance region. This phenomenon is associated with the orientation of chemical bonds at the interfaces in semiconductor-based heterostructures with the zinc blende structure.

So far, the interfacial anisotropy was studied in type II structures, where the exciton is„seated“ directly at the interface. In the studied structures with type I quantum wells, the exciton is not tied to a separate interface, but fills the whole well. Nevertheless, thanks to the barrier asymmetry, optical anisotropy of interfaces also appears in such wells. Exciton oscillator strength difference for two polarizations in these structures is comparable with the value observed in type II ZnSe/BeTe structures.

Another peculiarity of the studied spectra is associated with the fact that the birefringence effect on the exciton with a light hole (Figure 3) is considerably larger than that on the exciton with a heavy hole. But these are light holes that directly contact with the interfaces, and the heavy holes are primarily in the Coulomb field of the electron [9]. The wave functions of heavy holes are certainly somehow distorted as a result of barrier anisotropy, but do not directly touch the interface. Therefore, the birefringence effect on them is considerably lower.

Acknowledgments

The authors are grateful to L.E. Golub and E.L. Ivchenko for the useful discussions.

Conflict of interest

The authors declare that they have no conflict of interest.

References

[1] D.J. Dunstan, A.D. Prins, B. Gil, J.P. Faurie. Phys. Rev. B **44**, *8*, 4017 (1991).
[2] Comprehensive Guide on Organic and Inorganic Solar Cells. Fundamental Concepts to Fabrication Methods. A volume in Solar Cell Engineerin / Ed. Md. Akhtaruzzaman, Vidhya Selvanathan. ISBN 978-0-323-85529-7. Academic Press (2022).
[3] S. Kasap, P. Capper. Springer handbook of electronic and photonic materials. Springer Science & Business Media (2007).
[4] A.Z. Al-Attili, D. Burt, Z. Li, N. Higashitarumizu, F. Gardes, Ya. Ishikawa, Sh. Saito. Sci. Rep. **12**, 7465 (2022).
[5] A.V. Platonov, V.P. Kochereshko, E.L. Ivchenko, G.V. Mikhailov, D.R. Yakovlev, M. Keim, W. Ossau, A. Waag, G. Landwehr. Phys. Rev. Lett. **83**, *17*, 3546 (1999).
[6] O. Krebs, P. Voisin. PRL **77**, 1829 (1996).
[7] E.L. Ivchenko, A.A. Toropov, P. Voisin. FTT, **40**, 1925 (1998). (in Russian).
[8] E.L. Ivchenko, P.S. Kopiev, V.P. Kochereshko, I.N. Uraltsev, D.R. Yakovlev, S.V. Ivanov, B.Ya. Meltser, M .A. Kalitievsky. FTP **22**, *5*, 784 (1988).
[9] L.V. Kotova, D.D. Belova, R. Andre, H. Mariette, V.P. Kochereshko. FTP, **3**, 4803 (2023). (in Russian).
[10] L.V. Kotova, A.V. Platonov, V.N. Kats, V.P. Kochereshko, S.V. Sorokin, S.V. Ivanov, L.E. Golub. Phys. Rev. B **94**, 165309 (2016).
[11] L.V. Kotova, A.V. Platonov, V.N. Kats, S.V. Sorokin, S.V. Ivanov, R. Andre, V.E. Bugrov, V.P. Kochereshko. Phys. Status Solidi B-Basic Solid State Phys. **256**, *6*, 1800665 (2019).
[12] L.V. Kotova, A.V. Platonov, R. André, H. Mariette, V.P. Kochereshko, Phys. Rev. In press.
[13] E.L. Ivchenko. Optical Spectroscopy of Semiconductor Nanostructures. Alpha Sci. Int., Harrow, UK (2005).
[14] A.S. Gurevich, V.P. Kochereshko, A.V. Platonov, A. Vaag, D.R. Yakovlev, G. Landver. FTT **46**, *4*, 759 (2004). (in Russian).
[15] I.L. Aleiner, E.L. Ivchenko. Pis'ma v ZhETF **55** (662), (1992). (in Russian).
[16] E.L. Ivchenko, A.Yu. Kaminsky, I.L. Aleiner. JETP **89**, 753 (1993).

Translated by Ego Translating